Published in final edited form as:

Diabetologia. 2015 December ; 58(12): 2832–2842. doi:10.1007/s00125-015-3768-4.

Deletion of ARNT/HIF1β in pancreatic beta cells does not impair glucose homeostasis in mice, but is associated with defective glucose sensing ex vivo

Renjitha Pillai[1], **Sabina Paglialunga**[1], **Monica Hoang**[1], **Katelyn Cousteils**[1], **Kacey J. Prentice**[2], **Eric Bombardier**[3], **Mei Huang**[1], **Frank J. Gonzalez**[4], **A. Russell Tupling**[3], **Michael B. Wheeler**[2], and **Jamie W. Joseph**[1]

[1]School of Pharmacy, University ofWaterloo, Health Science Campus building A, room 4008, 10A Victoria Street South, Kitchener, ON, Canada N2G 1C5

[2]Department of Physiology, University of Toronto, Toronto, ON, Canada

[3]Department of Kinesiology, University of Waterloo, Waterloo, ON, Canada

[4]Laboratory ofMetabolism, National Cancer Institute, Bethesda,MD, USA

Abstract

Aims/hypothesis—It has been suggested that the transcription factor ARNT/HIF1β is critical for maintaining in vivo glucose homeostasis and pancreatic beta cell glucose-stimulated insulin secretion (GSIS). Our goal was to gain more insights into the metabolic defects seen after the loss of ARNT/HIF1β in beta cells.

Methods—The in vivo and in vitro consequences of the loss of ARNT/HIF1β were investigated in beta cell specific *Arnt/ Hif1 β* knockout mice (β-Arnt$^{fl/fl/Cre}$ mice).

Results—The only in vivo defects found in β-Arnt$^{fl/fl/Cre}$ mice were significant increases in the respiratory exchange ratio and in vivo carbohydrate oxidation, and a decrease in lipid oxidation. The mitochondrial oxygen consumption rate was unaltered in mouse β-*Arnt* ^{re} islets upon glucose stimulation. β-Arnt$^{fl/fl/Cre}$ islets had an impairment in the glucose- stimulated increase in Ca^{2+} signalling and a reduced insulin secretory response to glucose in the presence of KCl and diazoxide. The glucose-stimulated increase in the NADPH/$NADP^+$ ratio was reduced in β-*Arnt*$^{fl/fl/Cre}$ islets. The reduced GSIS and NADPH/$NADP^+$ levels in β-*Arnt*$^{fl/fl/Cre}$ islets could be rescued by treatment with membrane-permeable tricarboxylic acid intermediates. Small interfering (si)RNA mediated knockdown of ARNT/HIF1β in human islets also inhibited GSIS. These results

Contribution statement RP and JWJ performed some of the mouse and human islet studies and wrote the paper. SP and MHo helped with some of the in vivo and mouse islet studies. KC helped with the in vivo studies. MHu helped with some of the mouse islet studies. Evaluation of whole-body bioenergetics in mice using CLAMS was carried out in collaboration with ART and EB. Calcium and MMP measurements were carried out in collaboration with MBW and KJP. FJG helped with the conceptual design of the paper and provided the *Amt/Hiflβ* floxed mice. SP, MHo, KC, KJP, EB, MHu, FJG, ART and MBW helped with revising the paper. JWJ is responsible for the integrity of the work as a whole. All authors approved the final version of the paper.

Electronic supplementary material The online version of this article (doi:10.1007/s00125–015-3768–4) contains peer-reviewed but unedited supplementary material, which is available to authorised users.

Duality of interest The authors declare that there is no duality of interest associated with this manuscript.

suggest that the regulation of GSIS by the K_{ATP} channel-dependent and -independent pathways is affected by the loss of ARNT/HIF1 β in islets.

Conclusions/interpretation—This study provides three new insights into the role of ARNT/HIF1β in beta cells: (1) ARNT/HIF1β deletion in mice impairs GSIS ex vivo; (2) β-*Arnt*$^{fl/fl/Cre}$ mice have an increased respiratory exchange ratio; and (3) ARNT/HIF1β is required for GSIS in human islets.

Keywords

ARNT/HIF1β; Insulin release Metabolism; Pancreatic beta cell

Introduction

The transcription factor aryl hydrocarbon receptor nuclear translocator/hypoxia inducible factor-1β (ARNT/HIF1β) is important for a wide range of cellular functions, including the response to hypoxia, angiogenesis, placental development, and metabolism of xenobiotics [1]. It has also been suggested that ARNT/HIF1β might play a role in the pathogenesis of type 2 diabetes, in part because it has been identified as being required for maintaining beta cell function. ARNT/HIF1β has been found to be reduced by 90% in human type 2 diabetic islets, and is necessary to maintain normal in vivo glucose homeostasis and insulin secretion in mice [2].

While it is believed that ARNT/HIF1β plays a role in beta cell insulin secretion, the mechanisms by which it regulates beta cell function are not known. We previously found that a reduction of ARNT/HIF1β in 832/13 clonal beta cells led to a reduction in glucose utilisation, without affecting glucose oxidation or the ATP/ADP ratio [3]. Metabolic profiling of 832/13 cells deficient in ARNT/HIF1β also showed reduced levels of pyruvate and the tricarboxylic acid (TCA) cycle intermediates citrate/isocitrate, α-ketoglutarate, fumarate and malate, suggesting impaired anaplerosis. In the current study, a beta cell specific *Arnt/Hif1β* knockout mouse (β-*Arnt*$^{fl/fl/Cre}$) was generated to further assess the mechanisms by which ARNT/HIF1β regulates insulin secretion in beta cells, and how it leads to altered glucose homeostasis in vivo.

Methods

Reagents

All reagents and kits were obtained from Sigma (St Louis, MO, USA), unless otherwise specified.

Generation of beta cell specific β-*Arnt*$^{fl/fl/Cre}$ mice

β-*Arnt*$^{fl/fl/Cre}$ mice were generated using Cre-loxP technology, as described in the electronic supplementary material (ESM) Methods. Mice were fed the Teklad Mouse Breeder Diet (Diet no. 8626; Teklad Diets, Madison, WI, USA). Experiments involving animals were approved by the local ethics committee.

Real-time PCR

RNA was isolated using an Aurum Total RNA Mini Kit (Bio-Rad, Mississauga, ON, Canada). cDNA was synthesised using an iScript cDNA Synthesis Kit (Bio-Rad). Real-time PCR was performed using SsoFast EvaGreen Real-Time PCR Supermix (Bio-Rad). See ESM Table 1 for primer sequences.

Western blot

Hypothalamic and islet proteins were extracted using cell lysis buffer (Cell Signaling, Whitby, ON, Canada) containing phenylmethylsulfonyl fluoride (0.5 mmol/l), leupeptin (10 μg/ml), aprotinin (10 μg/ml) and pepstatin (5 μg/ml). Extracts (40 μg) were resolved on 10% Bis-Tris SDS polyacrylamide gels and electrotransferred to PVDF membranes (Life Technologies, Carlsbad, CA, USA). ARNT/HIF1β was detected using a rabbit antibody against ARNT/HIF1β (1:500; Cell Signaling), followed by HRP- conjugated anti-rabbit antibody (1:15,000) (Sigma). γ-Tubulin was detected by immunoblotting with a mouse antibody against γ-tubulin (1:4,000) (Sigma), followed by HRP-conjugated anti-mouse antibody (1:15,000) (Amersham, Piscataway, NJ, USA). Protein bands were detected using the ECL Advance immunoblot detection kit (Amersham).

IPGTT, insulin tolerance test, respiratory exchange ratio,

$\dot{V}O_2$ and $\dot{V}CO_2$ An intraperitoneal GTT was conducted and the respiratory exchange ratio (RER), volume of oxygen consumed ($\dot{V}O_2$) and volume of carbon dioxide produced ($\dot{V}CO_2$) were measured as described in the ESM Methods.

Islet isolation

Human islets were provided by the Alberta Diabetes Institute Islet Core at the University of Alberta in Edmonton (AB, Canada), with the assistance of the Human Organ Procurement and Exchange Program and the Trillium Gift of Life Network in procuring donor pancreases for research (islets were obtained from four donors with an average age of 60 years) [4, 5]. Experiments involving human islets were approved by the local ethics committee. Mouse islets were isolated and cultured as previously described [3, 6].

Cell lines

The 832/13 cell line [7], derived from INS-1 rat insulinoma cells [8], was used for some of these experiments. The cells were a gift from C. B. Newgard (Duke University, Durham, NC, USA) and were cultured as previously described [3, 6, 7, 9].

siRNA transfection and generation of adenoviruses expressing siRNAs against ARNT/HIF1β

Expression of ARNT/HIF1β was suppressed in 832/13 cells by the introduction of small interfering (si)RNA duplexes or adenoviruses, as described in the ESM Methods.

Islet content and secretion of insulin and human growth hormone

Cell and islet glucose-stimulated insulin secretion (GSIS) was measured as previously described [3,6,9]. For the KCl plus diazoxide studies, islets were pretreated for 1 h in KRB

with 2 mmol/l glucose, followed by the addition of either 2 or 12 mmol/l glucose with or without 30 mmol/l KCl and 200 μmol/l diazoxide for 1 h. For the dimethylmalate (DMM) and dimethyl α-ketoglutarate (DMαKG) studies, 10 mmol/l of each was added to freshly prepared KRB solution on the day of the assay. After the assay, the buffer was collected and assayed for insulin using the Coat-A-Count RIA kit (Siemens, Los Angeles, CA, USA) and assayed for human growth hormone (hGH) secretion using a specific kit (HGH Human ELISA Kit; Life Technologies). Islet insulin content was measured as previously described [10]. Islet lysates were also assayed for hGH content using a specific hGH assay (HGH Human ELISA Kit; Life Technologies).

Oxygen consumption

Oxygen consumption was measured using an XF24 Extracellular Flux Analyzer (Seahorse Bioscience, Billerica, MA, USA), as previously described [11], in either 832/13 cells (5×10^4 cells per well) or mouse islets (50 islets per well). On the day of the assay, cells were pretreated with 2 mmol/l glucose for 2 h. Oxygen consumption was then measured in response to: 2 mmol/l glucose; 8 mmol/l glucose; 5 μmol/l oligomycin; 50 μmol/l2,4-dinitrophenol (DNP) with 20 mmol/l pyruvate for cells or 5 mmol/l DMM + DMαKG for islets; and 5 μmol/l rotenone and 5 μmol/l myxothiazol.

Calcium and mitochondrial membrane potential imaging

Changes in intracellular calcium concentrations were assessed using Fura-2AM (Life Technologies) in dispersed islet cells as previously described [12]. Mitochondrial membrane potential (MMP) was quantified in islets using a mitochondrial-specific dye (rhodamine 123) as previously described [12].

NADPH and $NADP^+$ measurements

832/13 cell NADPH and $NADP^+$ levels were measured using a NADPH/$NADP^+$ quantification kit (MAK038; Sigma). Briefly, 832/13 cells were plated onto a six-well plate and transfected with either control siRNA or *Arnt/Hif1β* siRNA. After 72 h, cells were preincubated for 2 h with KRB containing 2 mmol/l glucose at 37°C, 5% CO_2. Cells were then treated with KRB containing either 2 or 16.7 mmol/l glucose for 1 h. Two wells of the six-well plate were pooled, and NADPH and $NADP^+$ were extracted and then quantified. Islet ATP, ADP, $NADP^+$ and NADPH levels were measured by HPLC as previously described [9].

Statistical analysis

All results are given as means ± SEM. Statistical significance was assessed using Student's *t* test or by one- or two-way ANOVA, followed by multiple comparisons with a Holm-Sidak correction.

Results

Generation of beta cell specific β-*Arnt*$^{fl/fl/Cre}$ mice

To study the role of ARNT/HIF1β in pancreatic beta cells, a Cre-loxP technique was used to specifically disrupt the *Arnt/Hif1β* gene in beta cells. The Cre-mediated recombination resulted in the beta cell specific deletion of exon 6 (confirmed by PCR on islet genomic DNA), which encodes the basic helix-loop-helix region of the ARNT/HIF1β protein (ESM Fig. 1a). Islet *Arnt/ Hif1β* mRNA was reduced by 73±4% in β-*Arnt*$^{fl/fl/Cre}$ islets and by 33± 15% in heterozygous islets compared with control mouse islets (ESM Fig. 1b). ARNT/HIF1β protein levels were also reduced by 79±6% in β-Arnt$^{fl/fl/Cre}$ islets (ESM Fig. 1c). A small amount of genomic DNA recombination (deletion of *Arnt/Hif1β* exon 6, data not shown) was found by PCR in the hypothalamus; however, neither *Arnt/Hif1β* mRNA (data not shown) nor protein (ESM Fig. 1c) levels were altered in the hypothalamus.

In vivo glucose homeostasis

The only significant difference seen in 16 h fasting blood glucose values was among male control mice vs control Cre mice, heterozygous mice and β-*Arnt*$^{fl/fl/Cre}$ mice (ESM Fig. 1d). Female fasting blood glucose levels did not significantly differ among the groups (ESM Fig. 1d). Fasting plasma NEFA levels also did not differ among control, control Cre, heterozygous or β-*Arnt*$^{fl/fl/Cre}$ female mice (ESM Fig. 3a). An IPGTT was performed on 15- to 20-week-old female and male mice after a 16 h fast. We did not find any differences during the IPGTT for male mice, and only control female mice had a significantly lower AUC as compared with control Cre, heterozygous and β-*Arnt*$^{fl/fl/Cre}$ mice (Fig. 1a-d). Plasma insulin levels from male mice during the IPGTT were not different from each other (Fig. 1e). Control female mice had a significantly higher plasma insulin AUC during the IPGTT compared with control Cre, heterozygous and β-*Arnt*$^{fl/fl/Cre}$ mice (Fig. 1f), which was consistent with the improved glucose levels during the IPGTT.

To assess insulin action, an i.p. insulin tolerance test (ITT) was conducted on both male and female mice. The only significant (but small) difference seen for the ITT was between male β-*Arnt*$^{fl/fl/Cre}$ mice vs heterozygous and control Cre mice (Fig. 2a-d).

Comprehensive metabolic assessment of β-*Arnt*$^{fl/fl/Cre}$ mice

The Comprehensive Lab Animal Monitoring System (CLAMS) was used to assess food intake, total activity, $\dot{V}O_2$ and $\dot{V}CO_2$ in 15–20-week-old male control Cre, heterozygous and β-*Arnt*$^{fl/fl/Cre}$ mice. All measurements were normalised to body weight and the mice had ad libitum access to food and water during the experiment. There were no significant differences seen in body weight (Fig. 3a), food intake (Fig. 3b) or total activity (Fig. 3c) in β-*Arnt*$^{fl/fl/Cre}$ mice compared with control Cre and heterozygous littermates. However, the RER, which is the ratio of $\dot{V}CO_2/\dot{V}O_2$, was significantly higher in β-*Arnt*$^{fl/fl/Cre}$ mice compared with control Cre littermates (Fig. 3d). An RER closer to 1 signifies preferential use of carbohydrates as an energy source, whereas an RER closer to 0.7 suggests a preference for the use of fat as an energy source. In support of these results, we found that β-*Arn*$^{fVfl/Cre}$ mice had significantly elevated whole-body carbohydrate oxidation (Fig. 3e) and

significantly lower lipid oxidation (Fig. 3f). These in vivo studies suggest that β-*Arnt*$^{fl/fl/Cre}$ mice do not have any significant impairment of glucose homeostasis.

Mouse islet studies

We next assessed whether islets from β-*Arnt*$^{fl/fl/Cre}$ mice had any defects in GSIS. Basal GSIS from both male and female β-*Arnt*$^{fl/fl/Cre}$ islets were not significantly different from each other, as compared with both control Cre islets and heterozygous islets (Fig. 4a-c). At 16.7 mmol/l glucose, islets from male β-Arnt$^{fl/fl/re}$ mice secreted 54±3% less insulin (Fig. 4a) and islets from female β-*Arnt*$^{fl/fl/re}$ mice secreted 67±10% less insulin (Fig. 4b), compared with control Cre islets. Male heterozygous mice secreted 24±5% less insulin as compared with control Cre mice (Fig. 4a). At 12 mmol/l glucose, islets from female β-*Arnt*$^{fl/fl/Cre}$ mice secreted significantly less insulin than both control Cre islets and those from heterozygous mice (Fig. 4b).

In order to assess where the defect lies in insulin secretion, we first determined islet insulin response to KCl and diazoxide. Diazoxide was used to hold K_{ATP} channels open and KCl was used to depolarise the beta cell membrane, which effectively clamps cytosolic calcium at an elevated level. At 2 mmol/l glucose, β-*Arnt*$^{fl/fl/Cre}$ islets secreted 44 ± 18% less insulin than control Cre islets in the presence of diazoxide and KCl (Fig. 4c), suggesting a possible defect in the K_{ATP} channel-dependent pathway that involves Ca^{2+} influx. At 12 mmol/l glucose, β-*Arnt*$^{fl/fl/Cre}$ islets secreted 49±6% less insulin as compared with control Cre islets in the presence of diazoxide and KCl (Fig. 4c), suggesting that ARNT/HIF1β also plays a role in regulating the K_{ATP} channel-independent pathway.

A key player in the K_{ATP} channel-independent pathway of insulin release is glucose-regulated anaplerosis. We have previously shown that ARNT/HIF1β regulates anaplerosis in clonal beta cells [3]. We next sought to rescue the defect in the K_{ATP} channel-independent pathway in β-*Arnt*$^{fl/fl/Cre}$ islets using the anaplerotic substrates DMM and DMαKG. At both low and high glucose, DMM and DMαKG rescued the de-fects seen in insulin secretion and in fact significantly in-creased GSIS in β-*Arnt*$^{fl/fl/Cre}$ islets as compared with control Cre islets (Fig. 4d). These results suggest that both the K_{ATP} channel-dependent and -independent pathways are altered by the loss of ARNT/HIF1fi, and that both can be rescued by supplementation with anaplerotic substrates. The studies performed in Fig. 4a-d were all done in the same experiment with replicates.

Recently, it has been shown that some of the commonly used beta cell expressing Cre lines that use either the rat or mouse insulin promoter might produce and secrete hGH [13]. One of the suggested lines to secrete hGH is the RIP-Cre mouse line, similar to the one used in this study. Several key findings from the previous study suggest that islets have elevated hGH content, and that secretion of hGH leads to activation of the prolactin receptor, increased insulin content and increased beta cell mass [13]. However, our RIP-Cremice did not secrete any detectable hGH and islets contained only a small amount of hGH in all lines assessed (<1% of the hGH content seen in [13]), including flox control (fl/fl/+) islets that do not express Cre (ESM Fig. 3a). Detection of hGH in control (fl/fl/+) islets suggests that the hGH kit used in our study and that of Brouwers et al [13] might be reacting with other islet

components besides hGH. We also found no significant differences in islet insulin content among any of the groups (ESM Fig. 3b).

Mitochondrial oxygen consumption rate in clonal 832/13 cells and β-*Arnt*$^{fl/fl/Cre}$ islets

We next looked at the oxygen consumption rate (OCR) in the absence of ARNT/HIF1β. There was a significant reduction in GSIS from 832/13 cells treated with 16.7 mmol/l glucose and an siRNA against ARNT/HIF1β ($p<0.05$; 254±24 (μU insulin/[mg protein] for control siRNA-treated cells vs 130±13 (μU insulin/[mg protein] for *Arnt*/*Hifl*/β siRNA-treated cells). However, there was no significant difference seen in the OCR of clonal 832/13 cells treated with an siRNA against ARNT/HIF1β in response to glucose, as compared with siRNA-treated control cells (Fig. 5a). ARNT/HIF1β was knocked down in the clonal 832/13 beta cell line by 76±5% in these studies. OCR was also not significantly different in β-*Arnt*$^{fl/fI/Cre}$ islets in response to glucose as compared with control islets (Fig. 5b, c). This suggests that the oxidative capacity was not reduced in cells that lacked ARNT/HIF1β. OCR in response to oligomycin (an ATP synthase inhibitor), DNP (a mitochondrial uncoupler) and rote- none and myxothiazol (electron transport chain inhibitors) were also not significantly affected in the clonal 832/13 cells or islets that lacked ARNT/HIF1β (Fig. 5). These results indicate that loss of ARNT/HIF1β does not lead to defects in mitochondrial respiration.

MMP in β-*Arnt*$^{fl/fl/Cre}$ islets

To further investigate the mechanism(s) underlying defective insulin secretion observed in β-*Arnt*$^{fl/fl/Cre}$ islets, MMP was measured using the mitochondrial-specific dye rhodamine 123. The addition of 20 mmol/l glucose resulted in the hyperpolarisation of the mitochondrial membrane to the same degree in both control Cre and β-*Arnt*$^{fl/fl/Cre}$ islets (Fig. 6a, b). The addition of 1 mmol/l sodium azide, a respiratory chain inhibitor, also resulted in the depolarisation of MMP to the same extent in both control and β-*Arnt*$^{fl/fl/Cre}$ islets. These data suggest that the loss of ARNT/HIF1β does not impact MMP.

Intracellular Ca^{2+} levels from β-Arnt$^{fl/fl/Cre}$ islets

To investigate whether the impairment in GSIS observed in β-*Arnt*$^{fl/fl/Cre}$ islets is due to changes in intracellular Ca^{2+} levels, we measured Ca^{2+} signalling in response to glucose. There was no difference seen in cytosolic Ca^{2+} levels at low glucose (2 mmol/l) in β-*Arnt*$^{fl/fl/Cre}$ islets as compared with control islets (Fig. 6c, d). However, upon stimulation with 20 mmol/l glucose, the AUC for intracellular Ca^{2+} levels was 6.5±0.7% lower in β-*Arnt*$^{fl/fl/Cre}$ islets compared with control Cre islets. Depolarisation of the plasma membrane with 30 mmol/l KCl in the presence of 20 mmol/l glucose also led to a significant reduction in the AUC for intracellular Ca^{2+} levels by 6.0±0.8% in β-*Arnt*$^{fl/fl/Cre}$ islets as compared with control Cre islets (Fig. 6c, d). The defects in Ca^{2+} signalling in β-*Arnt*$^{fl/fl/Cre}$ islets were delayed, with a peak delta difference of the normalised Ca^{2+} response 0.085±0.002 seen at 9 min (Fig. 6c). This indicates that the loss of ARNT/HIF1β leads to a reduction in glucose-induced Ca^{2+} influx.

Loss of ARNT/HIFlβ blocked the glucose-stimulated increase in the ATP/ADP ratio and led to a reduction in the NADPH/NADP+ ratio

Consistent with no effect on islet respiration in β-*Arnt*$^{fl/fl/Cre}$ islets, we found that there was no significant effect on low- and high-glucose-stimulated increases in the ATP/ADP ratio as compared with control Cre islets (Fig. 6e). However, unlike control Cre islets, β-*Arnt*$^{fl/fl/Cre}$ islets did not show a significant increase in the ATP/ADP ratio in response to high glucose (Fig. 6e). This suggests that the dynamic increase in the ATP/ADP ratio that is typically seen in islets is lost in β-*Arnt*$^{fl/fl/Cre}$ islets.

We next investigated a key signalling molecule generated in the κ_{atp} channel-independent pathway by anaplerosis, NADPH [3, 14–16]. The lack ARNT/HIF1β led to a loss of the glucose-stimulated increase in the NADPH/NADP$^+$ ratio in the clonal beta cell line 832/13 cells (ESM Fig. 2b) and in β-*Arnt*$^{fl/fl/Cre}$ islets (Fig 6f). The decrease in the NADPH/ NADP$^+$ ratio in β-*Arnt*$^{fl/fl/Cre}$ islets in response to glucose could be rescued by the addition of the TCA intermediates DMM and DMαKG (Fig. 6f). These results are consistent with a defect in the K_{ATP} channel-independent pathway in beta cells that lack ARNT/HIF1β.

Human islet insulin secretion

Knockdown of ARNT/HIF1β in human islets using siRNA adenoviruses (AdsiARNT1 and AdsiARNT2 targeted to two different regions in the *ARNT/HIF 1β* gene) resulted in a significant reduction in *ARNT/HiF1β* mRNA expression (AdsiARNT1 by 67±7% and AdsiARNT2 by 62±5%) and inhibited GSIS (Fig. 7).

Discussion

In the present study, we used pancreatic beta cell specific ARNT/HIF1β knockout mice to characterise the metabolic defects) seen in ARNT/HIF1β knockout islets. We show that ARNT/HIF1β is critical for maintaining the normal secretory function ofpancreatic beta cells in vitro. The β-*Arnt*$^{fl/fl/Cre}$ islets had defective K_{ATP} channel-dependent and -independent insulin secretion, which was associated with a reduction in glucose-stimulated changes in cytosolic calcium and in glucose-stimulated increases in the NADPH/NADP$^+$ ratio.

The defects in insulin secretion could be rescued by adding the TCA intermediates malate and α-ketoglutarate, which is consistent with our previous studies showing a defect in anaplerosis in ARNT/HIF1β knockout beta cells. Surprisingly, the only in vivo defect found in the β-*Arnt*$^{fl/fl/Cre}$ mice compared with control Cre mice (+/+/Cre) was a significantly higher RER, suggesting a preference for carbohydrate fuel utilisation; in addition, males had impaired insulin action. None of the male mouse lines showed a significant difference in IPGTT; however, female control floxed mice had higher in vivo insulin levels and an improved IPGTT than control Cre, heterozygous and β-*Arnt*$^{fl/fl/Cre}$ mice.

Interestingly, male β-*Arnt*$^{fl/fl/Cre}$ mice had defective insulin action and increased RER. The increased RER in male β-*Arnt*$^{fl/fl/Cre}$ mice suggests an in vivo preference for using carbohydrates as a fuel, and one possible reason for this is changes in key metabolic tissues. The main metabolically active insulin-sensitive tissues are the liver and skeletal muscle [17].

Changes in fuel preferences in these two tissues can have dramatic effects on whole-body metabolism [18]. However, plasma glucose, plasma NEFA, food intake, total activity level, fat-pad size (data not shown) and body weight were similar in β-*Arnt*$^{fl/fl/Cre}$ and control Cre mice, suggesting that any changes in fuel preference in these tissues do not affect a number of key in vivo variables. It has been suggested that a sedentary lifestyle increases RER values and decreases sensitivity to insulin [19–21]. In this scenario, mice would tend to accumulate more fat. This possibility also does not fit with our β-*Arnt*$^{fl/fl/Cre}$ mouse phenotype, as these mice had normal levels of total activity and fat-pad size.

Another possible cause of these changes in insulin action and RER is a loss of ARNT/HIF1β in the hypothalamus. Although we found that there was a small amount of genomic recombination of ARNT/HIF1β in the hypothalamus, these changes did not result in any differences in *Arnt/Hiflβ* mRNA or protein levels in the hypothalamus. It is possible that looking at whole-hypothalamic changes in ARNT/HIF1β might not fully capture events in a small subset of neurons with altered ARNT/HIF1β levels. The altered subset of neurons is unlikely to be the pro-opiomelanocortin (POMC) neurons, as deletion of ARNT/HIF1β in this population of neurons has been reported to have dramatic effects on obesity [22]. At this point, we do not know why there are changes in insulin action and RER in β-*Arnt*$^{fl/fl/Cre}$ mice, and this is an active area of research. However, it is intriguing to speculate that the insulin-producing hypothalamic neurons might be involved in these changes.

Our results with isolated islets from β-*Arnt*$^{fl/fllCre}$ mice clearly indicate that ARNT/HIF1β plays a role in the metabolic regulation of insulin secretion. We have also shown that siRNA-mediated knockdown of ARNT/HIF1β in human islets also inhibits GSIS. Our studies demonstrate that the two signals critical for insulin secretion—rises in the NADPH/$NADP^+$ ratio and intracellular Ca^{2+}—are key players regulated by ARNT/HIF1β. As previously shown by our group, loss of ARNT/HIF1β in 832/13 cells leads to a decrease in the glucose-induced rise in TCA cycle intermediates [3]. We have now shown that this loss of anaplerosis is associated with a reduction in the glucose-stimulated rise in the NADPH/$NADP^+$ ratio, and that we can rescue insulin release and the loss of NADPH/$NADP^+$ signalling by replenishing the TCA intermediates. In addition to its role in regulating anaplerosis and NADPH, ARNT/HIF1β also regulates Ca^{2+} signalling in beta cells. This appears to be dependent on the role of ATP in cells that lack ARNT/HIF1β. Our results are consistent with those of another study in which siRNA- mediated knockdown of ARNT/HIF1β was associated with inhibited GSIS, reduced glucose-stimulated plasma membrane depolarisation and reduced K_{ATP} channel activity in INS1 clonal cells [23].

One possible regulator of ARNT/HIF1β fi is carbohydrate- responsive element-binding protein (ChREBP). It has been shown that the ChREBP is a negative regulator of *Arnt/Hif1β* gene expression in mouse islets [24]. Thus, elevated glucose levels could lead to an increase in ChREBP transcriptional activity and reduced ARNT/HIF1β levels. This could provide one mechanism by which chronically elevated glucose (glucotoxicity) could inhibit insulin release. This possibility is currently being investigated in the laboratory.

There are some differences between our study and that of Gunton et al [2], which also looked at the role of ARNT/HIF1β. This might be due to a number of factors, the most

important ofwhich is that we used two controls (+/+/Cre and fl/fl/+ mice), whereas the Gunton study used only fl/fl/+ mice as the primary control [2]. Other possible differences could include different diets, gut microbiota, genetic back-grounds and the extent of ARNT/HIF1β knockout. Another less likely possibility for the differences seen between the two studies is that the RIP-Cre strains used might have had unique phenotypes. This issue with the RIP-Cre mouse line arose after the publication of the Gunton et al study in 2005 [2], and thus revisiting these results is critical to moving forward with our understanding of the role of ARNT/HIF 1β in insulin secretion and diabetes. It has recently been shown that some beta cell specific Cre lines might express and secrete hGH [13]. However, we could not find any detectable release of hGH from any of the islet groups in this study, and could only detect about 1% of the total hGH islet content found in the Brouwers et al study in islets expressing fl/fl/+ and RIP-Cre [13]. Overall, hGH does not seem to be playing as big a role in the RIP-Cre mouse line as it does in the pdx1-Cre^{late} mouse line, and is unlikely to have been a factor in the current study.

In conclusion, ARNT/HIF1βplays a key role in maintaining the secretory function of pancreatic beta cells, mainly through the regulation of calcium signalling, anaplerosis and the NADPH/NADP^{+} ratio. The in vivo role of ARNT/HIF1β is more controversial and requires further investigation. As the ARNT/HIF1β knockout islets have defective insulin secretion in vitro, it is likely that these animals might be predisposed to developing diabetes if stressed, for example with a high-fat diet.

Supplementary Material

Refer to Web version on PubMed Central for supplementary material.

Acknowledgments

Funding This work was supported by Canadian Institute of Health Research (CIHR) grants to JWJ (FRN 86638) and MBW (MOP-324754), and by a Natural Sciences and Engineering Research Council of Canada (NSERC) and Canadian Diabetes Association doctoral scholarship to RP KJP is supported by a CIHR doctoral research award.

Abbreviations

ARNT/	Aryl hydrocarbon receptor nuclear translocator/
HIF1β	hypoxia inducible factor-1 β
ChREBP	Carbohydrate-responsive element-bindingProtein
DMαKG	Dimethyl α-ketoglutarate
DMM	Dimethylmalate
DNP	2,4-Dinitrophenol
GSIS	Glucose-stimulated insulin secretion
hGH	Human growth hormone
IPGTT	Intraperitoneal GTT

ITT	Insulin tolerance test
MMP	Mitochondrial membrane potential
OCR	Oxygen consumption rate
RER	Respiratory exchange ratio
siRNA	Small interfering RNA
TCA	Tricarboxylic acid
$\dot{V}\mathbf{CO_2}$	Volume of carbon dioxide produced
$\dot{V}\mathbf{O2}$	Volume of oxygen consumed

References

1. Kewley RJ, Whitelaw ML, Chapman-Smith A (2004) The mammalian basic helix-loop-helix/PAS family of transcriptional regulators. Int J Biochem Cell Biol 36:189–204 [PubMed: 14643885]
2. Gunton JE, Kulkarni RN, Yim S et al. (2005) Loss of ARNT/HIF1β mediates altered gene expression and pancreatic-islet dysfunction in human type 2 diabetes. Cell 122:337–349 [PubMed: 16096055]
3. Pillai R, Huypens P, Huang M et al. (2011) Aryl hydrocarbon receptor nuclear translocator/hypoxia-inducible factor-1β plays a critical role in maintaining glucose-stimulated anaplerosis and insulin release from pancreatic β-cells. J Biol Chem 286:1014–1024 [PubMed: 21059654]
4. Korbutt GS, Elliott JF, Ao Z, Smith DK, Warnock GL, Rajotte RV (1996) Large scale isolation, growth, and function of porcine neonatal islet cells. J Clin Invest 97:2119–2129 [PubMed: 8621802]
5. Kin T, Shapiro AM (2010) Surgical aspects of human islet isolation. Islets 2:265–273 [PubMed: 21099323]
6. Huypens P, Pillai R, Sheinin T et al. (2011) The dicarboxylate carrier plays a role in mitochondrial malate transport and in the regulation of glucose-stimulated insulin secretion from rat pancreatic beta cells. Diabetologia 54:135–145 [PubMed: 20949348]
7. Hohmeier HE, Mulder H, Chen G, Henkel-Rieger R, Prentki M, Newgard CB (2000) Isolation of INS-1-derived cell lines with robust ATP-sensitive K+ channel-dependent and -independent glucose-stimulated insulin secretion. Diabetes 49:424–430 [PubMed: 10868964]
8. Asfari M, Janjic D, Meda P, Li G, Halban PA, Wollheim CB (1992) Establishment of 2-mercaptoethanol-dependent differentiated insulin-secreting cell lines. Endocrinology 130:167–178 [PubMed: 1370150]
9. Patterson JN, Cousteils K, Lou JW, Manning Fox JE, MacDonald PE, Joseph JW (2014) Mitochondrial metabolism of pyruvate is essential for regulating glucose-stimulated insulin secretion. J Biol Chem 289:13335–13346 [PubMed: 24675076]
10. Joseph JW, Jensen MV, Ilkayeva O et al. (2006) The mitochondrial citrate/isocitrate carrier plays a regulatory role in glucose-stimulated insulin secretion. J Biol Chem 281:35624–35632 [PubMed: 17001083]
11. Malmgren S, Nicholls DG, Taneera J et al. (2009) Tight coupling between glucose and mitochondrial metabolism in clonal β-cells is required for robust insulin secretion. J Biol Chem 284:32395–32404 [PubMed: 19797055]
12. Joseph JW, Koshkin V, Saleh MC et al. (2004) Free fatty acid- induced β-cell defects are dependent on uncoupling protein 2 ex-pression. J Biol Chem 279:51049–51056 [PubMed: 15448158]
13. Brouwers B, de Faudeur G, Osipovich AB et al. (2014) Impaired islet function in commonly used transgenic mouse lines due to human growth hormone minigene expression. Cell Metab 20: 979–990 [PubMed: 25470546]

14. Ronnebaum SM, Ilkayeva O, Burgess SC et al. (2006) A pyruvate cycling pathway involving cytosolic NADP-dependent isocitrate dehydrogenase regulates glucose-stimulated insulin secretion. J Biol Chem 281:30593–30602 [PubMed: 16912049]
15. Jensen MV, Joseph JW, Ronnebaum SM, Burgess SC, Sherry AD, Newgard CB (2008) Metabolic cycling in control of glucose- stimulated insulin secretion. Am J Physiol Endocrinol Metab 295: E1287–E1297 [PubMed: 18728221]
16. Huypens PR, Huang M, Joseph JW (2012) Overcoming the spatial barriers of the stimulus secretion cascade in pancreatic β-cells. Islets 4:1–9 [PubMed: 22143007]
17. Wang Z, Ying Z, Bosy-Westphal A et al. (2010) Specific metabolic rates of major organs and tissues across adulthood: evaluation by mechanistic model of resting energy expenditure. Am J Clin Nutr 92:1369–1377 [PubMed: 20962155]
18. Muoio DM, Newgard CB (2008) Mechanisms of disease: molecular and metabolic mechanisms of insulin resistance and β-cell failure in type 2 diabetes. Nat Rev Mol Cell Biol 9:193–205 [PubMed: 18200017]
19. Rimbert V, Boirie Y, Bedu M, Hocquette JF, Ritz P, Morio B (2004) Muscle fat oxidative capacity is not impaired by age but by physical inactivity: association with insulin sensitivity. FASEB J 18:737–739 [PubMed: 14977873]
20. Morio B, Hocquette JF, Montaurier C et al. (2001) Muscle fatty acid oxidative capacity is a determinant of whole body fat oxidation in elderly people. Am J Physiol Endocrinol Metab 280:E143–E149 [PubMed: 11120668]
21. Smorawinski J, Nazar K, Kaciuba-Uscilko H et al. (2001) Effects of 3-day bed rest on physiological responses to graded exercise in athletes and sedentary men. J Appl Physiol (1985) 91: 249–257 [PubMed: 11408437]
22. Zhang H, Zhang G, Gonzalez FJ, Park SM, Cai D (2011) Hypoxia- inducible factor directs POMC gene to mediate hypothalamic glucose sensing and energy balance regulation. PLoS Biol 9:e1001112 [PubMed: 21814490]
23. Kim JS, Zheng H, Kim SJ et al. (2009) Role of aryl hydrocarbon receptor nuclear translocator in KATP channel-mediated insulin secretion in INS-1 insulinoma cells. Biochem Biophys Res Commun 379:1048–1053 [PubMed: 19141293]
24. Noordeen NA, Khera TK, Sun G et al. (2010) Carbohydrate- responsive element-binding protein (ChREBP) is a negative regulator of ARNT/HIF-1β gene expression in pancreatic islet β-cells. Diabetes 59:153–160 [PubMed: 19833882]

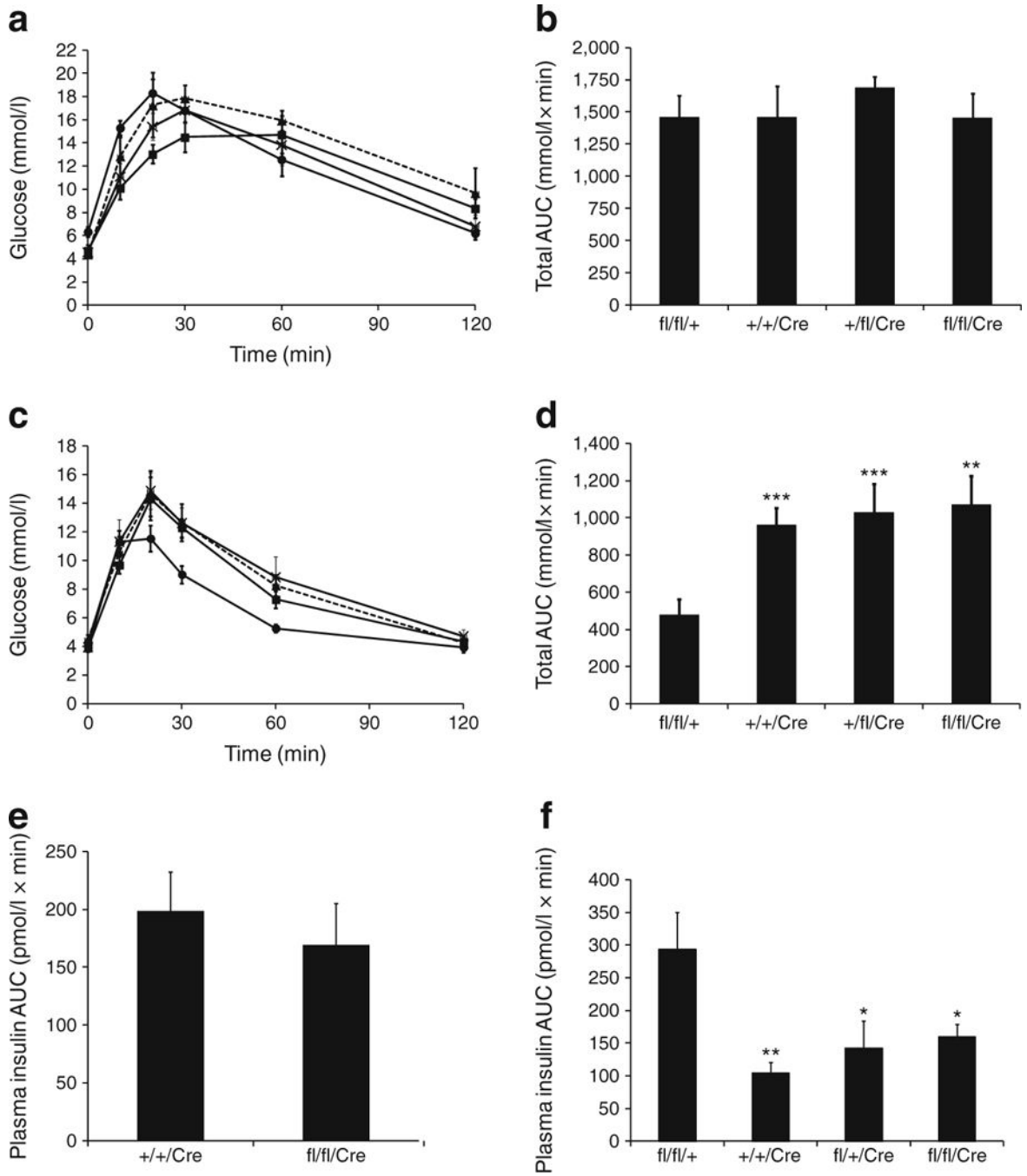

Fig. 1.

IPGTT measurements. (**a**) IPGTT in male mice. (**b**) AUC of (**a**). (**c**) IPGTT in female mice. (**d**) AUC of (**c**). (**e**) Male plasma AUC insulin levels during the IPGTT of (**a**). (**f**) Female plasma AUC insulin levels during the IPGTT of (**c**). fl/fl/+, control mice (circles), +/+/Cre, control Cre mice (squares), +/fl/Cre, heterozygous mice (triangles) and fl/fl/Cre, β-$Arnt^{fl/fl/Cre}$ mice (crosses). *p<0.05, **p<0.01, ***p<0.001 for+/+/Cre, fl/+/Cre or fl/fl/Cre vs fl/fl/+. n=9–12 per genotype for both males and females. Data are means ± SEM

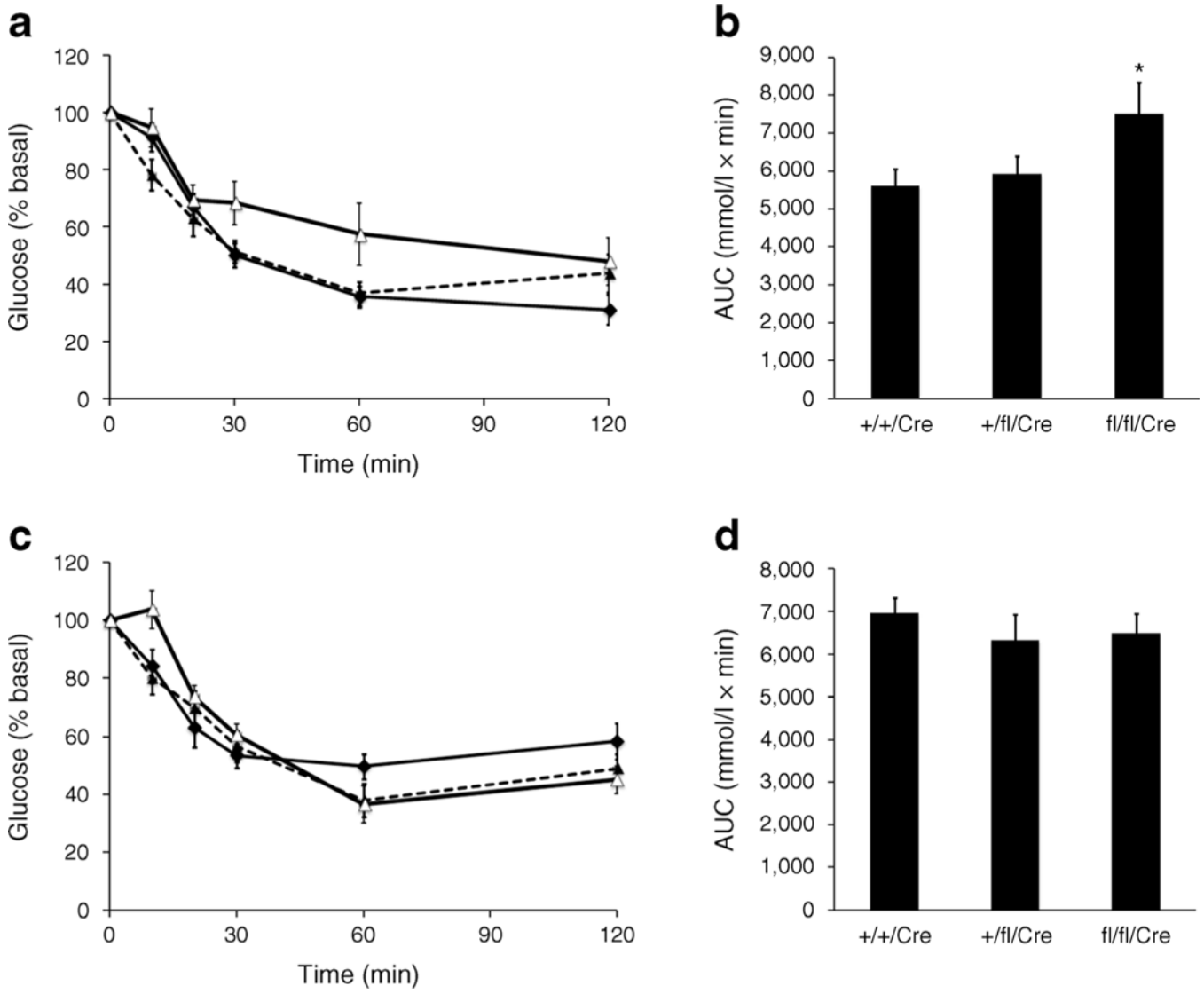

Fig.2.

ITT measurements. (**a**) ITT in male mice using 1.5U insulin/(kg mouse weight). (**b**)AUC of (**a**). (**c**) ITT in female mice using 1.2 U insulin/ (kg mouse weight). (**d**) AUC of (**c**). +/+Cre, control Cre mice (diamonds//0, +/fl/Cre, heterozygous mice (black triangles) and β-*Arnt*$^{fl/flCre}$ mice (fl/fl/Cre, white traingles). * p< 0.05 control Cre mice (+/+/Cre) vs β-*Arnt*$^{fl/fl/Cre}$ mice (fl/fl/Cre). n =9–12 per genotype for ITT. Data are means ± SEM

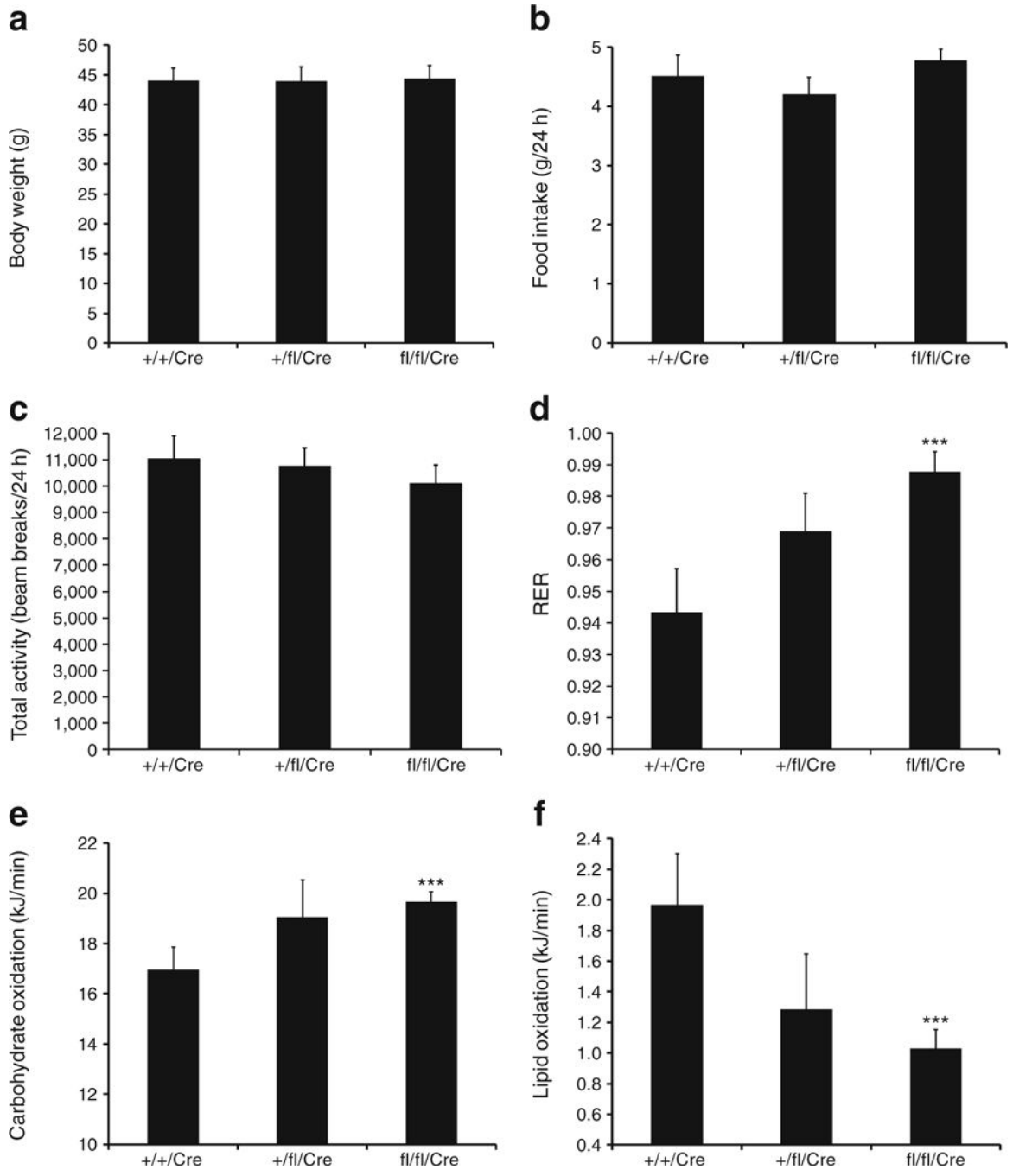

Fig. 3.

Indirect calorimetry measuremetns ofmale con troll Cre(+/+/Cre), heterozygous (+/fl/Cre) and β-*Arntl*$^{fl/fl/Cre}$ mice. (**a**) Body weight, (**b**) food intake, (**c**) total activity, (**d**) RER, (**e**) whole-body carbohydrate oxidation and (**f**) whole-body lipid oxidation. ***p<0.001 for β-*Arnt*$^{fl/fl/Cre}$ mice vs control Cre mice. n = 9. Data are means ± SEM

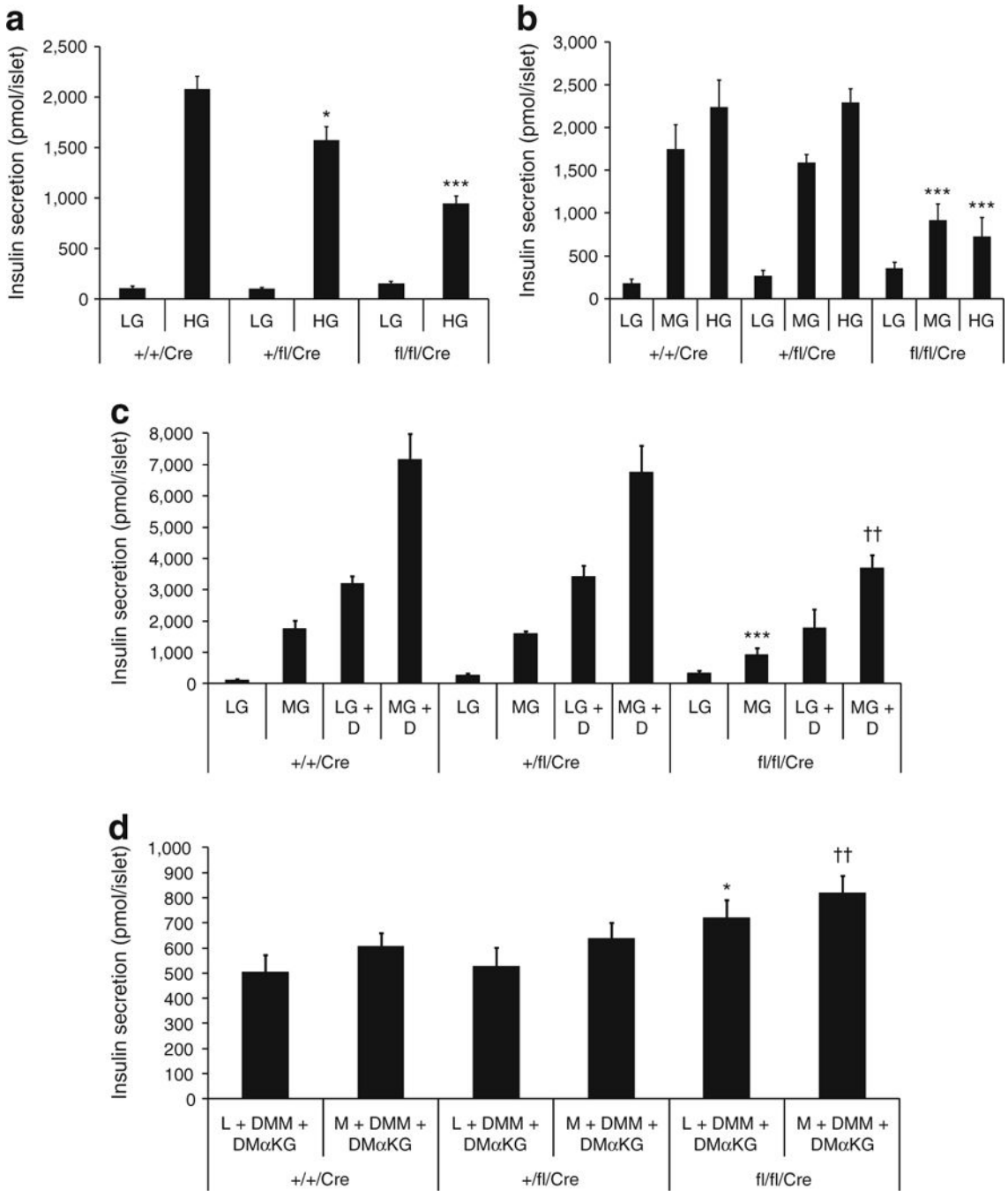

Fig. 4.

GSIS from islets. **(a)** GSIS from male Cre control (+/+/Cre), heterozygous (+/fl/Cre) and β-*Arnt*$^{fl/fl/Cre}$ (fl/fl/Cre) islets in response to low (2 mmol/l; LG) and high (16.7 mmol/l; HG) levels of glucose. **(b)** GSIS from female Cre control (+/+/Cre), heterozygous (+/fl/Cre) and β-*Arnt*$^{fl/fl/Cre}$ (fl/fl/Cre) islets in response to LG, medium glucose (12 mmol/l; MG) and HG. **(c)** GSIS from female Cre control (+/+/Cre), heterozygous (+/fl/Cre) and β-*Arnt*$^{fl/fl/Cre}$ (fl/fl/Cre) islets in response to LG or MG, with or without 30 mmol/l KCl and 200 μmol/l diazoxide (D). Data are means ± SEM of eight to 10 independent experiments. *p <0.05 for

HG +/fl/Cre vs HG control Cre islets; ***p<0.001 for MG or HG β-*Arnt*$^{fl/fl/Cre}$ islets vsMG or HG control Cre islets; $^{\dagger\dagger}p$<50.01 for MG+D β-*Arnt*$^{fl/fl/Cre}$ islets vs MG+D control Cre islets. **(d)** GSIS from female Cre control (+/+/Cre), heterozygous (+/fl/Cre) and β-*Arnt*$^{fl/fl/Cre}$ (fl/fl/ Cre) islets in response to 2 mmol/l glucose (L) or 8 mmol/l glucose (M), both plus 10 mmol/l DMM and 10 mmol/l DMαKG. *p<0.05 for L+DMM+DMαKG β-*Arnt*$^{fl/fl/Cre}$ islets vs L+DMM+DMαKG female control Cre islets; $^{\dagger\dagger}p$<0.01 for M+DMM +DMαKG β-*Arnt*$^{fl/fl/Cre}$ islets vsM+DMM+DMαKG female control Cre islets.Data aremeans ± SEM of 3–6 independent experiments

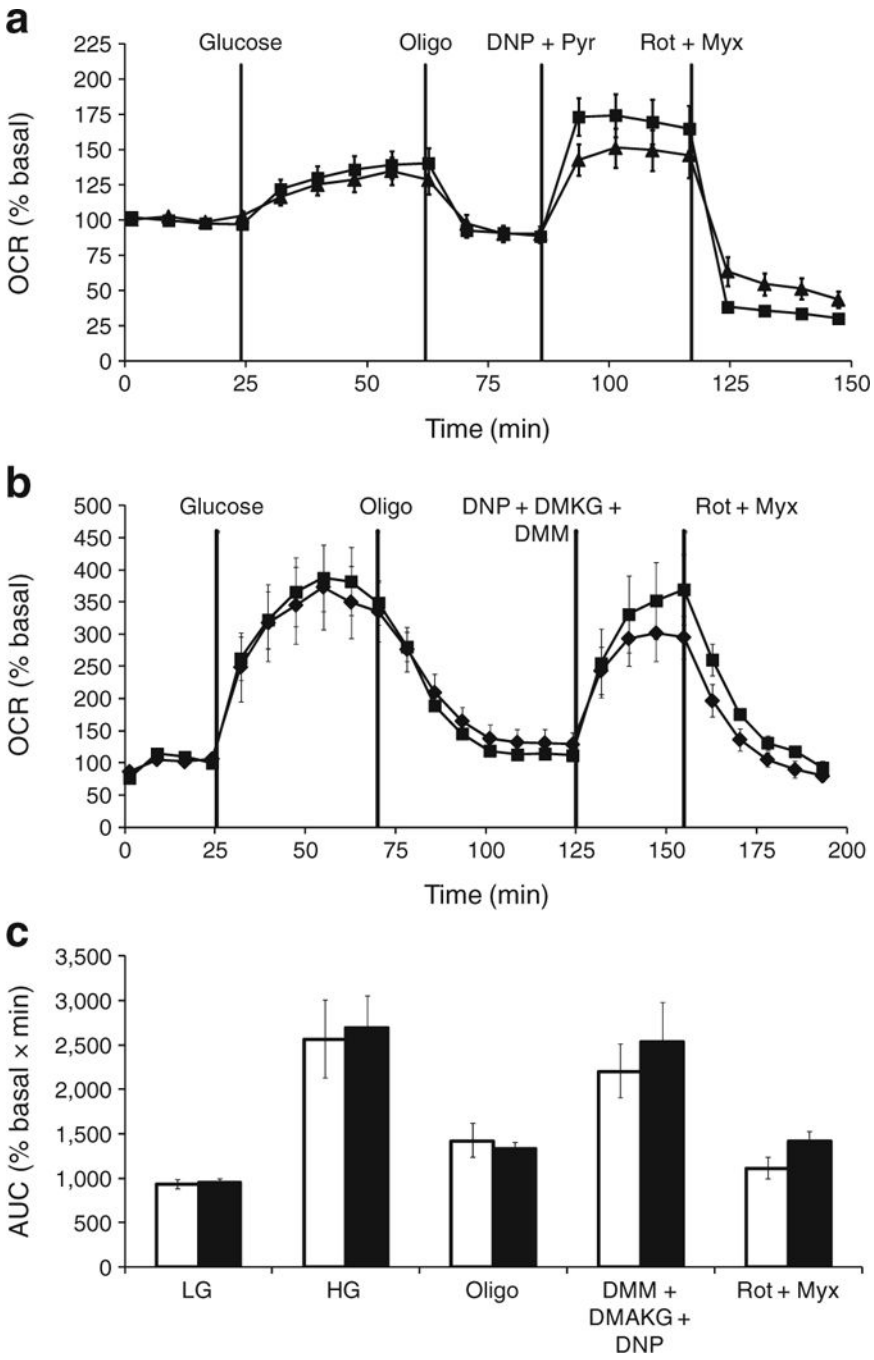

Fig. 5.

Mitochondrial OCR in 832/13 clonal beta cells and β-*Arnt*$^{fl/fl/Cre}$ islets. **(a)** Clonal 832/13 cells treated with either an siRNA control (squares) or siRNAs targeting ARNT/HIF1β (triangles) (**a**) or β-*Arnt*$^{fl/fl/Cre}$ islets (**b, c**; control Cre (+/+/Cre) diamonds, β-*Arnt*$^{fl/fl/Cre}$ squares) were assessed for the OCR in response initially to 2 mmol/l glucose, followed by the sequential addition of 16.7 mmol/l glucose (Glucose); 5 μmol/l oligomycin (Oligo); 50 μmol/l DNP plus either 20 mmol/l pyruvate (Pyr; for clonal 832/13 cells) or 5 mmol/l DMM and DMαKG (for islet studies); and 10 μmol/l each of rotenone (Rot) and myxothiazol

(Myx). For (**a**) and (**b**), values are expressed as per cent basal OCR. (c) AUC of (b) (white bars, +/+/Cre; black bars, β-*Arnt*$^{fl/fl/Cre}$). Four independent experiments were conducted for the siRNA-treated cells. For islet experiments, data are means ± SEM of 3–4 independent experiments

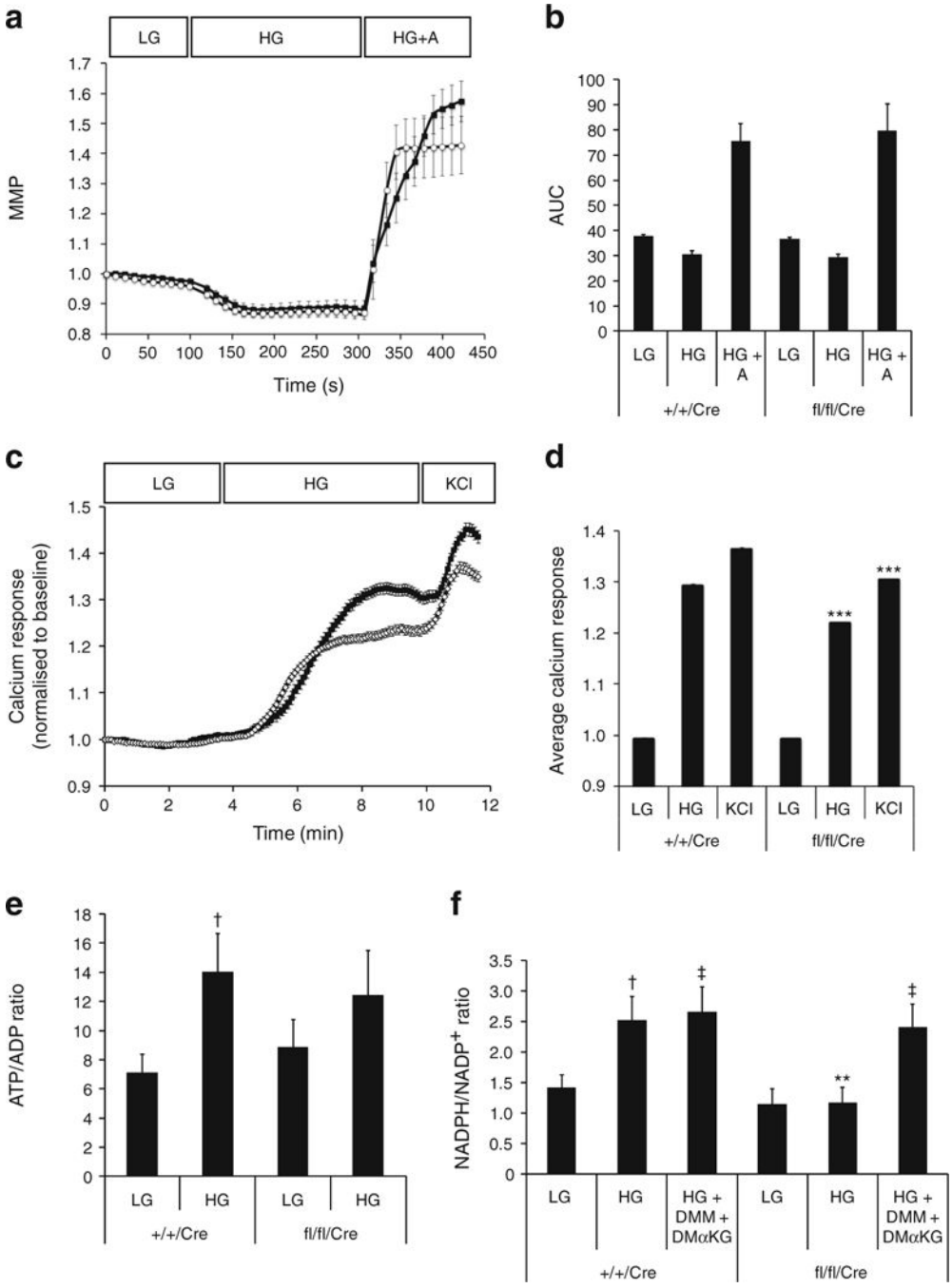

Fig. 6.

MMP, Ca^{2+} dynamics and the NADPH/$NADP^+$ ratio in β-*Arnt*$^{fl/fl/Cre}$ islets. (**a**) MMP was assessed using rhodamine 123. Average fluorescent signals (normalised to baseline) of Cre control (+/+/Cre; black squares) and β-*Arnt*$^{fl/fl/Cre}$ (white circles) islets in response to 2 mmol/l glucose (LG), 20 mmol/l glucose (HG) and 20 mmol/l glucose plus sodium azide (HG+A) (n=4 mice per group, with a minimum of 50 islets per mouse). (**b**) AUC of (**a**) (normalised response × s). (**c**) Intracellular Ca^{2+} levels were measured with Fura-2 AM (Life Technologies). Average normalised baseline fluorescent response for Cre control (+/+/ Cre;

black squares) and β-*Arnt*$^{fl/fl/Cre}$ (white diamonds) islets to 2 mmol/l glucose (LG), 20 mmol/l glucose (HG) and 20 mmol/l glucose plus 30 mmol/l KCl (KCl). (**d**) Average calcium response of (**c**). LG average 0–2.1 min; HG average 6.8–9.1 min; KCl average 10–12 min. Data are means ± SEM of three independent experiments. (**e**) ATP/ADP ratio in islets in response to 2 mmol/l glucose (LG) and 16.7 mmol/l glucose (HG) (n=10). (f) NADPH/NADP+ ratio in islets in response to 2 mmol/ l glucose (LG), 16.7 mmol/l glucose (HG) or 16.7 mmol/l glucose (HG) plus 10 mmol/l DMM and 10 mmol/l DMαKG (n=8–10). **p<0.01, ***p<0.001 for HG β-Arntfl/fl/Cre islets vs HG control Cre islets. $^{\dagger}p$<0.05 for HG vs LG control Cre (+/+/Cre) islets. $^{\ddagger}p$<0.05 for HG + DMM + DMαKG vs LG control Cre (+/+/Cre) or β-Arnt$^{fl/fl/Cre}$ islets

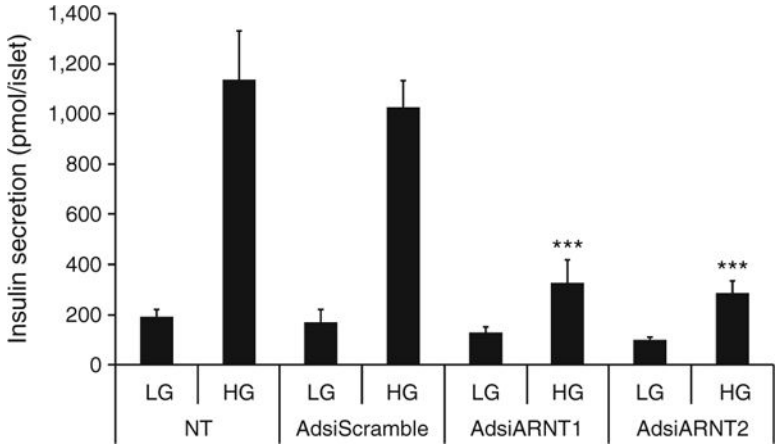

Fig. 7.

GSIS from human islets with reduced ARNT/HIF1β. GSIS from control no-treatment (NT), control adenoviral si (Adsi)Scramble or AdsiARNT1/2-treated human islets in response to 2 mmol/l (LG) or 16.7 mmol/l (HG) glucose (n=8). ***p<0.001 for HG AdsiARNT1/2-treated vs HG AdsiScramble islets